J Mol Model (2012) 18:3847–3856
DOI 10.1007/s00894-012-1384-5

ORIGINAL PAPER

Theoretical studies on the interaction of biphenyl inhibitors with *Mycobacterium tuberculosis* protein tyrosine phosphatase MptpB

Lihua Dong · Junyou Shi · Yongjun Liu

Received: 27 August 2011 / Accepted: 15 February 2012 / Published online: 11 March 2012

Abstract MptpB is an essential secreted virulence factor for *M. tuberculosis*. Inhibition of MptpB impairs mycobacterial survival in host macrophages and thus helps reduce tuberculosis infections. However, the binding mode of the biphenyl inhibitors, which are known as some of the most potent MptpB inhibitors, remains unclear. In this study, to understand the interactions between biphenyl inhibitors and MptpB, docking and molecular dynamics simulations were carried out using AutoDock and GROMACS softwares. Calculation results show that all the biphenyl inhibitors can be docked to the binding site of MptpB, with the acid warheads forming a hydrogen bond network at the active site. But the binding modes of other terminals of these inhibitors are different. The cyclohexyl and trifluoromethyl substituents at R1 and R2 sites are necessary for the inhibitors to adopt their double-site binding mechanism. The estimated binding affinities are basically consistent with the experimental results. MD simulations show that these binding complexes display different stability.

Keywords Tyrosine phosphatase B · Biphenyl inhibitor · Interaction · Molecular docking · Molecular dynamics simulation

Electronic supplementary material The online version of this article (doi:10.1007/s00894-012-1384-5) contains supplementary material, which is available to authorized users.

L. Dong · J. Shi · Y. Liu (✉)
Key Laboratory of Adaptation and Evolution of Plateau Biota,
Northwest Institute of Plateau Biology,
Chinese Academy of Sciences,
Xining,
Qinghai 810001, China
e-mail: yongjunliu_1@sdu.edu.cn

L. Dong
School of Chemical Engineering, Taishan Medical University,
Taian,
Shandong 271000, China

L. Dong
Graduate University of Chinese Academy of Science,
Beijing 100049, China

Introduction

Tuberculosis (TB) is a common but in some cases deadly infectious disease caused by *Mycobacterium tuberculosis*. TB typically attacks the lungs of the body and causes nearly 2 million deaths every year [1]. Currently, the standard treatment of TB uses a combination of different antibiotics that target a number of metabolic processes in mycobacteria, which requires typically 6–9 months to fully eradicate the infection. The emergence of multidrug-resistant strains during long-term treatment highlights the need for new drug targets to fight TB infection [2].

The success of *M. tuberculosis* is attributed largely to its ability to survive and replicate in macrophage phagosomes. The bacteria manipulate the host defense system and inhibit the normal process of phagosomes maturation into phagolysosomes, thereby preventing the acidification of lysosome contents and bacterial destruction [3, 4]. The *M. tuberculosis* genome encodes two phosphatases, termed MptpA and MptpB [5]. MptpB is an essential secreted virulence factor that functions in human macrophages [6, 7], and disruption of the MptpB gene severely impairs the ability of the mutant strains to survive in both IFN (interferon)-γ activated macrophages and guinea pigs [7]. It is reported that MptpB subverts the innate immune response by blocking the ERK1/2 (extracellular signal-regulated kinase1/2) and p38 (mitogen-activated protein p38) mediated IL-6 (interleukin 6) production

and promoting host cell survival by activating the protein kinase pathway [8]. The role of MptpB in pathogenesis suggests that MptpB is a potential new drug target for *M. tuberculosis*, and inhibition of MptpB could impair intracellular mycobacterial survival within macrophages and assist in clearing the infection [4].

Two crystal structures of MptpB have so far been determined with inorganic phosphate at the active site and in complex with inhibitor oxalylamino-methylene-thiophene sulfonamide (OMTS) [9, 10]. MptpB is a classical phosphatase (PTP) that contains structural elements reminiscent of dual-specificity phosphatases [11]. In addition to a highly conserved PTP active site, the enzyme contains a unique two-helix lid domain (α7 and α8, Fig. S1 in supporting information) that likely serves to protect the catalytic cysteine from oxidative inactivation. The biological substrates of MptpB have not yet been defined. The X-ray structure shows that two OMTS molecules bind to the protein, one in the active site (P1 site) and the other in the secondary binding site (P2 site) [9]. As a result, drug discovery efforts have focused on the identification of bidentate inhibitors capable of binding to both binding sites [4, 12]. Many MptpB inhibitors with different levels of inhibition and selectivity have been reported in the last few years [8, 12–16], but most of them contain at least two acidic sites or have higher molecular weight leading to poor cellular permeability.

By using a new fragment-based method called substrate activity screening (SAS), Soellner and co-workers recently identified a series of nonpeptidic MptpB inhibitors with low molecular weight [8, 17, 18]. Each of these inhibitors contains the same biphenyl substrate but a different phosphate mimetics warhead (Fig. 1). These biphenyl inhibitors proved to have submicromolar affinities for MptpB, and to be selective against MptpA and human PTPs [17]. Furthermore, development of these inhibitors revealed that ortho substituents at the R1 site are preferred for optimal binding, whiles the cyclohexyl group provides the most favorable enzyme interactions. With the acid warhead changing from isoxazole carboxylic acid (ISO) to isothiazolidinone (IZD) and difluoromethylphosphonic acid (DFMP), the binding affinities of these inhibitors change only a little.

Although experimental studies provide useful informations on the structure–activity relationship of biphenyl inhibitors, their binding modes and interaction details still remain unclear. Furthermore, so far there are no theoretical reports on the dynamic behavior of MptpB upon binding inhibitors. Thus, in this paper we present a docking and molecular dynamics simulation investigation aiming to understand the interaction details of biphenyl inhibitors with

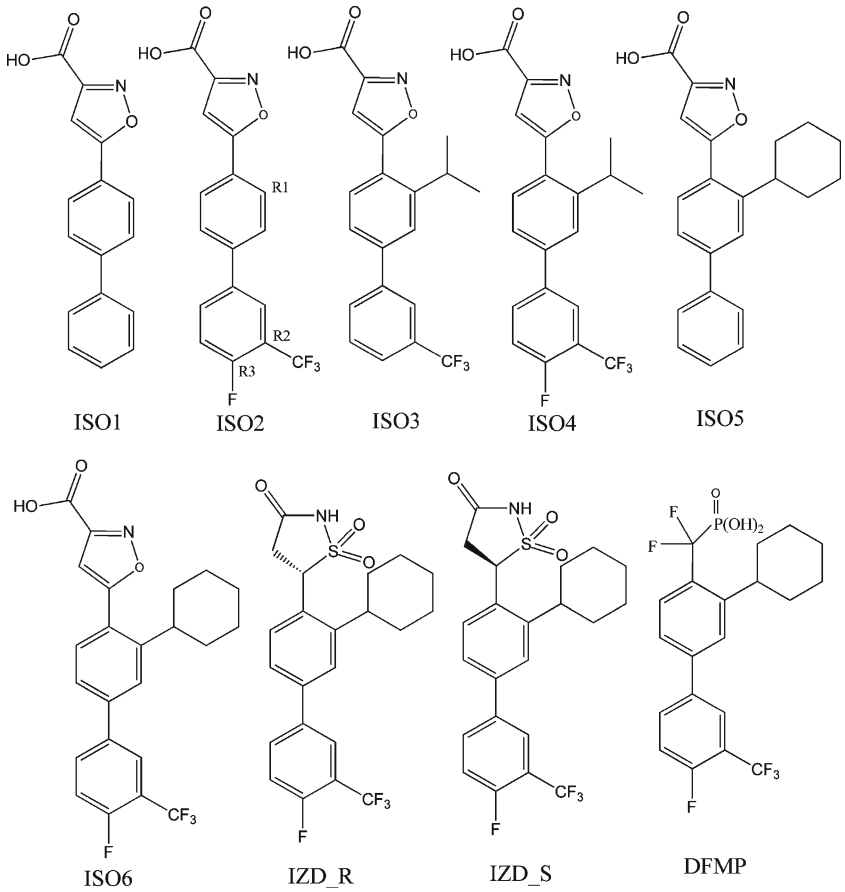

Fig. 1 Structures of biphenyl inhibitors

MptpB, and to explore the inhibitory mechanism of these inhibitors. We expect these results to be helpful in the design of new inhibitors.

Methods

Most of the biphenyl inhibitors used in this study were selected from experiments by Matthew [17, 18]. To explore the influence of different substitutes on binding modes and affinities, we also designed two inhibitors, ISO1 and ISO5. The Becke-3-parameter-Lee-Yang-Parr hybrid density functional theory at 6-31G(d) level implemented in the Gaussian03 package [19] was used to optimize the geometries of these inhibitors.

The 2.0 Å resolution crystal structure of MptpB in complex with inhibitor OMTS (PDB ID: 2OZ5) was used in the present study. This structure contains two almost identical chains, of which chain A was selected for docking experiments. Before docking, the ligand and crystallographic waters were deleted and missing residues were added using the MODELLER-9v7 program [20]. The ionization states of all residues were set at their default protonation states at neutral pH [21]. The complex was minimized in vacuum to relieve the possible steric clashes; then the prepared structure was used for docking studies.

Automated docking setup

Docking was performed with AutoDock 4.0 software [22, 23]. When docking, the protein MptpB was kept rigid, while all the torsional bonds of each ligand were set free. A grid of 60×60×60 points was generated with grid spacing of 0.375 Å around the active site. Polar hydrogens were added by using the Hydrogens module in AutoDock Tools (ADT). After that, Kollman united atom partial charges were assigned. For each complex, 100 independent docking runs were conducted. Module settings parameters were as follows [24–26]: population size of 150, a maximum number of 25 million energy evaluations, a maximum number of generations of 27,000, a crossover rate of 0.8 and a mutation rate of 0.02. The Solis and Wets method was applied to local search with a maximum of 300 iterations. The probability of performing a local search on an individual in the same population was 0.06, and the maximum number of consecutive success or failures before doubling or halving the step size of the local search was 4. Based on a root-mean-square deviation (RMSD) criterion of 1.0 Å, the docking results were clustered.

Molecular dynamics simulation setup

The docking results were used as the starting structure for MD simulation. The calculation was performed with the GROMACS program [27, 28] using AMBER99 force field [29–31]. Each complex was placed in the center of a 70 Å×70 Å×70 Å cubic box with periodic boundary conditions and solvated by TIP3P water molecules. Na^+ counterions were added to satisfy the electroneutrality condition. Berendsen temperature coupling and Parrinello-Rahman pressure coupling were used to keep the system in a stable environment (300 K, 1 bar), and the coupling constants were set to 0.1 ps. The partial mesh Ewald (PME) algorithm was employed to calculate long-range electrostatic interactions with a cutoff value of 1.0 nm, and a cutoff of 1.4 nm was set for van der Waals interactions. The LINCS algorithm [32] for bond constrains was applied. Each system was energy-minimized with a steepest-descent algorithm for 1,000 steps; then the solvent, ions and ligand were equilibrated for 100 ps in NTP and NVT ensembles, respectively, while heavy atoms of protein were restrained by a harmonic constraint with a force constant equal to 1,000 kJ mol^{-1} nm^{-2}. Finally, all the restraints were removed and a 10 ns MD simulation was performed for each system, except for MptpB/ISO6 (a system with 30 ns MD simulation). All the trajectories were stored every 10 ps for further analysis.

Results and discussion

Docking

The docking conformations for each biphenyl inhibitor were divided into groups according to a 1.0 Å RMSD criterion. Other than ISO6, which adopts two competitive conformations, other ligands mainly take one preponderant binding conformation (over 80%). Besides RMSD cluster analysis, Autodock also ranks the conformations in terms of binding energies. Energy items calculated by AutoDock include intermolecular energy (which is constituted by Van der Waals energy, hydrogen bonding energy, desolvation energy, and electrostatic energy), internal energy, and torsional energy. The sum of intermolecular energy and torsional energy is binding energy (Table 1). By comparing the binding energy with the experimental inhibition constant (K_i) of each inhibitor, we can see a good correlation between them, i.e., the lower the binding energy, the better the inhibitory activity. A detailed analysis is shown in the following sections.

ISO inhibitors

All the studied biphenyl inhibitors contain different acid warheads; according to the warheads, the inhibitors are named as isoxazole carboxylic acid (ISO) inhibitors, isothiazolidinone (IZD) inhibitors and difluoromethylphosphonic acid (DFMP) inhibitor, as shown in Fig. 1. ISO inhibitors were selected first to study the influence of different substituents on binding mode.

Table 1 Comparison of binding energies[a] (kcal mol^{-1}) and inhibition constants (K_i) of biphenyl inhibitors

Ligands	Intermolecular energies	Electrostatic energies	Torsional energies	Binding energies	Inhibition Constant (K_i)[b] μM(298.15 K)
ISO1	-8.08	-1.50	0.89	-8.69	
ISO2	-8.46	-1.43	1.19	-8.70	2.50±0.26
ISO3	-9.62	-1.50	1.49	-9.63	0.85±0.09
ISO4	-9.73	-1.41	1.49	-9.65	0.50±0.02
ISO5	-10.21	-1.03	1.19	-10.05	
ISO6_a	-10.46	-1.27	1.49	-10.24	0.22±0.03
ISO6_b	-10.12	-1.54	1.49	-10.18	
DFMP	-9.76	-1.97	1.49	-10.23	0.69±0.21
IZD_R	-10.45	-0.38	1.19	-9.63	2.4±0.0
IZD_S	-9.87	-0.49	1.19	-9.17	8.0+0.4

[a]Binding energy is the sum of the intermolecular energy and torsional energy

[b]The experimental K_i of ISO2, ISO3, ISO4 and ISO6 are from [17], and those of others are from [18]

Figure 2a shows that ISO1 molecule anchors into the binding pocket constituted by M206, F98, I203 and the P-loop. The carboxylate of the isoxazole head forms four H-bonds with residues C160, D165 and R166, and the oxygen atom in isoxazole ring forms another H-bond with the side chain of catalytic K164. The biphenyl structure extends to the hydrophobic channel consisting of F161, L199, M206 and F98.

Inhibitors ISO2, ISO3 and ISO4 adopt a binding mode similar to that of ISO1; the superimposition of their docking conformations is shown in Fig. 2e. The isoxazole heads of these ligands almost overlap. By comparing ISO1 with ISO2, we can see that the trifluoromethyl at the R2 position affects binding energies only slightly, as shown in Table 1. Similarly, ISO3 and ISO4 indicate that fluoro substitution at the R3 position shows no obvious influence on binding affinities, which is consistent with experimental results. However, when the R1 position of ISO2 was substituted by isopropyl (as shown in ISO3), the binding energy decreases markedly, which may be attributed to the increased hydrophobic interactions with hydrophobic residues L232, V231 and F98 (see Table S1 of Supporting information).

The binding conformation of ISO5 is shown in Fig. 2b. Comparing with ISO1, when a cyclohexyl group is introduced at the R1 position, the binding mode changes clearly. Due to the strong steric hindrance of cyclohexyl, the H-bond between the oxygen atom of the isoxazole ring and K164 is broken, and the isoxazole ring rotates with a new H-bond formed between the nitrogen atom and residue A162. But the strong H-bonds between carboxylate and the P-loop remain unchanged.

Experiments revealed that ISO6 represents the most potent inhibitor [17], which correspond to the lowest binding energy in our docking study. But, unlike other inhibitors, ISO6 exhibits two competitive docking conformations, named ISO6_a and ISO6_b, as shown in Fig. 2c,d, f. The binding mode of ISO6_a is similar to that of ISO5, and the isoxazole head still forms five H-bonds with residues C160, D165, R166 and A162. The cyclohexyl group locates inside the hydrophobic pocket formed by L232, V231 and L199, and the terminal phenyl interacts with the benzene ring of F98 through π–π interactions. However, the polar trifluoromethyl at the R2 position orients to hydrophobic residues I207 and M206, which may decrease the binding stability.

Different from ISO6_a, the substituted trifluoromethyl of ISO6_b extends to the positively charged residues R63, R64 and R210 (the P2 site of MptpB), forming strong electrostatic interactions with these residues (Fig. 2d). The carboxylate of the isoxazole head still forms four strong H-bonds with the surrounding residues, while the nitrogen atom of isoxazole forms a weak H-bond (3.323 Å) with K164. This suggests that ISO6_b adopts a double-site binding conformation with the acid warhead at the P1 site and the trifluoromethyl group extending to the P2 site. The H-bond strength of ISO6_b is relatively weaker (four strong H-bonds plus one weak H-bond) than that of ISO6_a (five strong H-bonds). But the electrostatic and Van der Waals interactions of ISO6_b are stronger (see Table 1) than that of ISO6_a. Consequently, ISO6_a and ISO6_b have similar binding energies in spite of their different binding modes.

To sum up, all the ISO inhibitors use their isoxazole moieties bound at the P1 active site. However, with the change of substituents on biphenyl backbone, the binding conformations of other termini differ. Single replacement by trifluoromethyl at the R2 position or fluoro at the R3 position influences the binding energy only slightly. But big and hydrophobic substituents at the R1 position facilitate ligand binding. Only when R1 and R2 are replaced by cyclohexyl and trifluoromethyl synchronously, can inhibitors adopt the double-site binding mode, and the binding energy decreases obviously, which is consistent with the experimental results of Matthew [17].

DFMP and IZD inhibitors

DFMP is a phosphate isostere that can be introduced in place of the isoxazole group. Despite being dianionic, the DFMP isostere was shown by Merck to be cell permeable and orally bioavailable in animals [33]. The docking conformation of

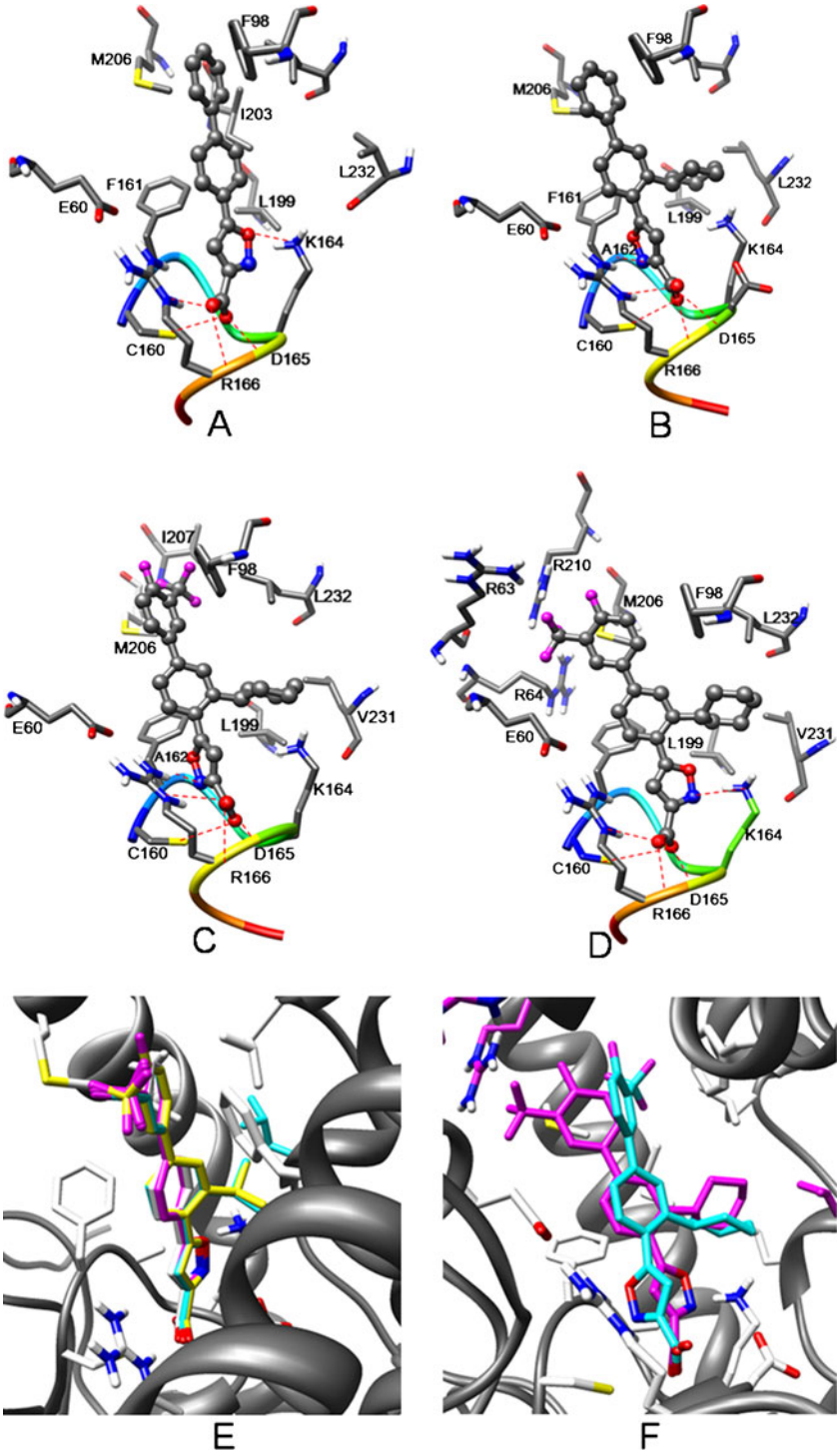

Fig. 2 Docking conformations of MptpB complexed with isoxazole carboxylic acid (ISO) inhibitors. The active site (P-loop) is shown in *ribbon*. The *dotted lines* represent H-bonds. **a** ISO1; **b** ISO5; **c** ISO6_a; **d** ISO6_b; **e** Superimposition of docking results of ISO1 to ISO4: *white* ISO1, *magenta* ISO2, *green* ISO3, *yellow* ISO4; **f** Superimposition of docking results of ISO6_a and ISO6_b: *magenta* ISO6_a, *green* ISO6_b

DFMP inhibitor shown in Fig. 3a shows that the substituted trifluoromethyl and cyclohexyl adopt a similar orientation and binding mode to that of ISO6_b. The dianionic phosphate makes one characteristic hydrogen bonded ion pair with the buried side chain of R166, and three normal H-bonds with R166, C160 and D165, which is in accordance with the phosphate in crystal structure (1YWF). Furthermore, the two substituted fluoro atoms (F1 and F2 as shown in Fig. 3a) form strong polar interactions with the positively charged side chain of K164. Compared with ISO6_b, the H-bond interactions between DFMP and the protein decrease, but electrostatic interactions increase (Table 1).

IZD inhibitor has two enantiomers: IZD_R and IZD_S. Rawls [18] proposed that MptpB binds one IZD enantiomer preferentially, but this was difficult to pick out experimentally. The binding conformations of these two enantiomers are

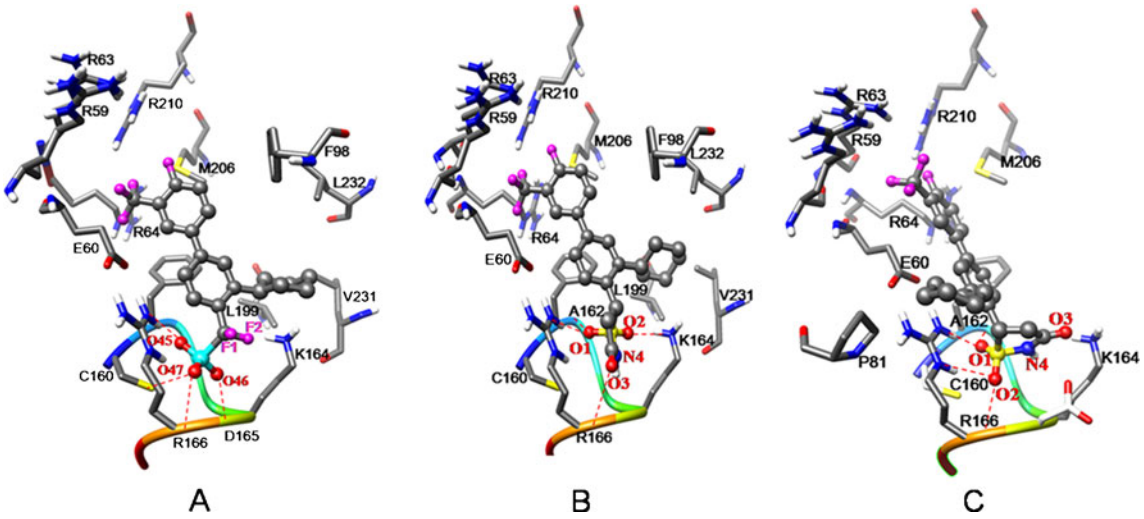

Fig. 3 Docking conformations of MptpB complexes with difluoromethylphosphonic acid (DFMP) and isothiazolidinone (IZD) inhibitors. (**a**) DFMP; (**b**) IZD_R and (**C**) IZD_S

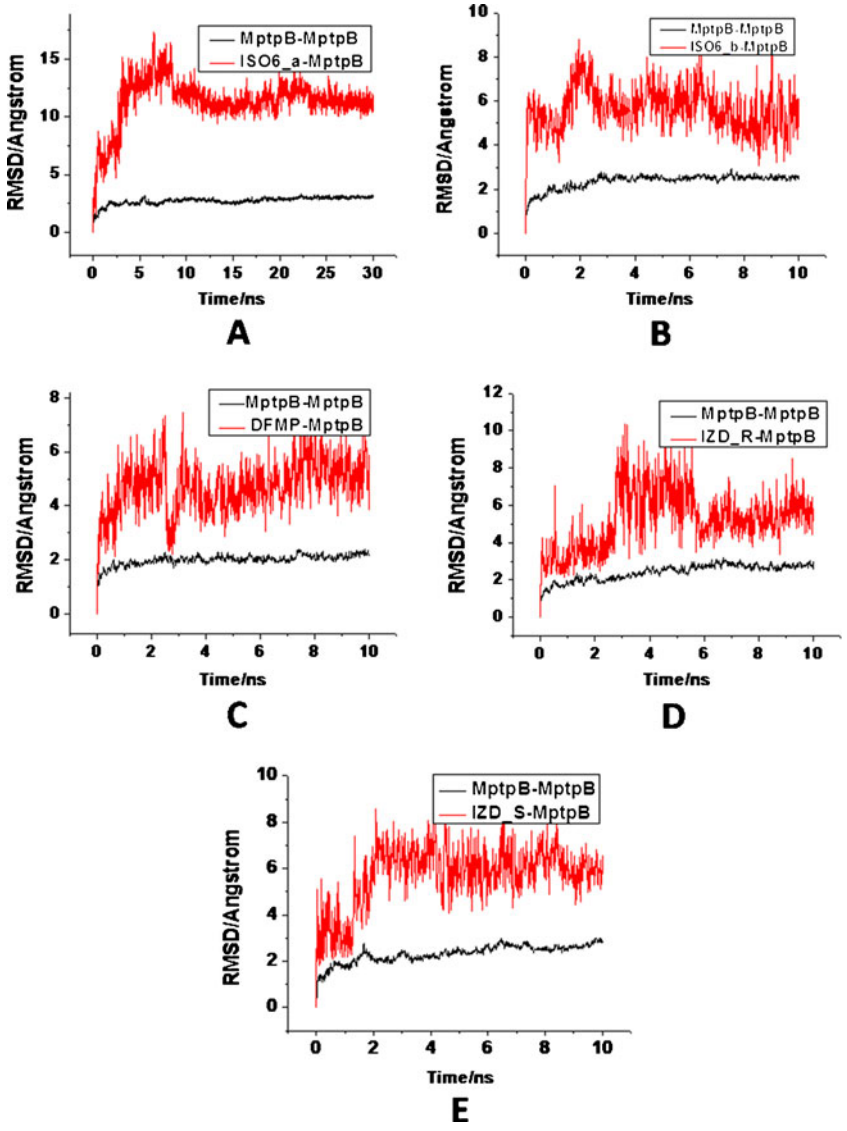

Fig. 4 Time dependence of root-mean-square deviation (RMSD) from molecular dynamic (MD) simulations

shown in Fig. 3b and c, from which we can see that their binding modes and binding energies are quite different. As shown in Fig. 3b, IZD_R adopts a double-site binding mode with the trifluoromethyl extending to the P2 binding site and IZD forming four H-bonds with residues A162, K164 and R166. The substituted cyclohexyl locates in the hydrophobic pocket formed by L232, V231 and L199. Compared with IZD_R, the interactions between IZD_S and the P-loop are rearranged. The sulfonyl group of IZD_S forms four H-bonds with A162 and R166 (Fig. 3c). The carbonyl oxygen atom points to the positively charged residue K164. This binding mode of the IZD moiety makes the cyclohexyl group close to polar residues (such as P81 and E60) and far from the hydrophobic specialty pocket, causing a remarkable decrease in binding affinity.

Based on the docking results we can conclude that the preferential enantiomer must be IZD_R, which has lower binding energy and represents a more potent enantiomer.

Molecular dynamics simulations

In order to explore the stabilities and dynamic characteristics of MptpB complexed with biphenyl inhibitors, we carried out MD simulations based on docking conformations. ISO6_a, ISO6_b, DFMP, IZD_R and IZD_S complexes were selected as representative. The RMSDs of ligand relative to MptpB, and MptpB relative to its original conformation were calculated and outlined in Fig. 4, which indicate that all five systems reached equilibrium within the simulation time, and the enzyme stabilized at a mean RMSD value of 2.0 Å, but the RMSDs of each inhibitor are very different.

Figure 4a shows that the RMSD of ISO6_a relative to MptpB increases within the first 10 ns and then stabilizes at about 12 Å. By checking the interval conformations, we note that the binding mode of ISO6_a has already changed. The trifluoromethyl group shows significant instability during simulation. The hydrophobic and polar interactions push trifluoromethyl out of its original hydrophobic binding pocket and close to the polar residues Lyp99 and Arg210. These enhanced polar interactions cause a rearrangement of the ISO moiety. The original H-bond between A162 and the nitrogen atom is broken and the isoxazole rotates toward the side chain of K164. Due to their strong interactions, the H-bonds between carboxylate and the P-loop are stable during simulation. The substituted cyclohexyl is always in the hydrophobic pocket. The MD average structure of ISO6_a is very similar to the docking conformation of the ISO6_b complex.

Figure 4b gives the RMSD of ISO6_b relative to the protein. This system approaches equilibrium at the beginning of the MD simulation and the RMSD is maintained at about 5 Å, suggesting a stable binding of ISO6_b with MptpB. During the simulation, several water molecules enter the binding pocket and interact with the protein or inhibitor, which is consistent with the experimental results [10]. By checking the interval conformations using VMD, we find that the weak H-bond between the nitrogen atom and the side chain of K164 vanished and is substituted by two strong water-bridged H-bonds with the O5 atom (see Fig. 5). This bridged water molecule exits during all the simulation time and plays an assistant role in the binding of the ligand.

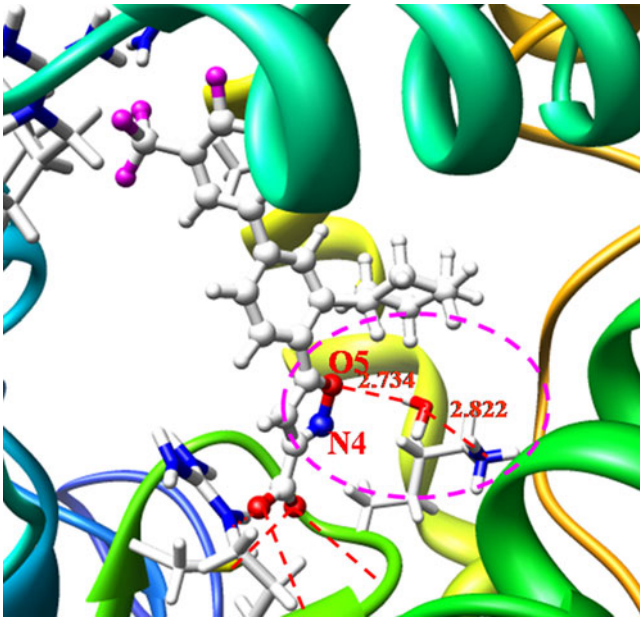

Fig. 5 Average structure of MptpB/ISO6_b complex derived from MD simulation. *Dotted lines* H-bonds (lengths in Ångstroms)

Figure 4c shows similar curves as Fig. 4b, indicating that DFMP inhibitor also binds stably to the enzyme. This can be confirmed by checking the H-bonds between the phosphate moiety and residues in the active site (Fig. S2). The slight fluctuation in H-bonds length is due to the slight fluctuations of active site residues in their equilibrium position.

The RMSDs of IZD_R and IZD_S complexes are given in Fig. 4d and e. The RMSD of IZD_R shows a sudden increase from 3 ns to 6 ns, and stabilizes at 5 Å. By checking the distance between sulfonyl oxygen atoms and related residues (see Fig. S3), we find that the RMSD curve of IZD_R

Table 2 Binding affinities[a] (in pK_i units) of the ligands calculated by Xscore based on conformations from docking and MD simulation

Ligand	Docking	MD simulation
ISO6_a	7.30	7.51
ISO6_b	7.45	7.53
DFMP	7.38	7.55
IZD_R	7.16	7.24
IZD_S	6.66	6.75

[a] Average binding affinities from HPScore, HMScore and HSScore

correlates with the rotation of sulfonyl and the slight change of side chain of K164. The average conformation of the last 4 ns takes the original binding mode. Figure 4e indicates that the RMSD of IZD_S is higher than that of IZD_R, which is due partly to the instability of cyclohexyl in its polar surroundings. However, owing to the large steric hindrance, cyclohexyl cannot rotate in the hydrophobic pocket. Furthermore, one water molecule enters the binding pocket and makes an H-bond bridge between the N4-atom and the side chain of K164, while the H-bond interactions between sulfonyl and the active site exit in the whole simulation time, implying the relative dynamic stability of IZD_S complex.

Our dynamics study shows that these biphenyl inhibitors can bind steadily to MptpB. With the exception of ISO6_a, the MD results of the complexes exhibit similar binding modes. The RMSDs of inhibitors to MptpB (5–8 Å) are relatively higher, which may be attributed to the movement of the trifluorometyl and associated phenyl backbone. To examine how these results affect the binding affinities for these inhibitors after MD simulation, we calculated the binding affinities for the average structures derived from the last 2 ns using the program X-score (Table 2) [34]. Compared with the corresponding results obtained by docking structures, we find that all these inhibitors exhibit more or less improved binding affinities after MD simulation. Furthermore, the binding affinities of the two OMTS molecules binding to MptpB (PDB ID: 2OZ5) at the P1 and P2 sites are calculated to be 7.92 and 6.96 (unit in pK_i) respectively, indicating that OMTS is comparable with these bidentate inhibitors from a binding affinity point of view.

The crystal structure of MptpB:PO4 represents a closed state of the two-helix lid domain (α7 and α8), and that of the inhibited MptpB:OMTS complex indicates a relative open state [9, 10]. By using single-molecule FRET measurements, Flynn et al. [35] found asynchronous movements of the two lid helices in MptpB. Our study also detects the rearrangement of the lid domain during MD simulations (as shown in Fig. 6). The movement of helix α7 reoriented the side chain of R210 and, consequently, made a slight rotation of the trifluoromethyl and its connected phenyl due to the strong electrostatic interactions.

Conclusions

In this study, we performed docking and MD simulation studies to explore the inhibitory mechanism of biphenyl inhibitors toward MptpB. The docking results indicate that, except for ISO6, these biphenyl inhibitors adopt mainly one binding conformation with MptpB. Among the interactions between MptpB and inhibitors, the H-bond interaction is the most important. All these inhibitors with their acid warheads form H-bond networks at the active site (P1 site). The hydrophobic interactions between R1 substitutes and some hydrophobic residues can affect the inhibition specialty to some extent. Furthermore, when R1 and R2 sites are substituted synchronously by cyclohexyl and trifluoromethyl, such as in ISO6_b, DFMP and IZD inhibitors, the trifluoromethyl orients to the positively charged binding pocket (P2 site) and makes strong electrostatic interactions with residues R59, R64 and R210, which indicates a double-site binding mechanism. Compared with other bidentate inhibitors, the biphenyl inhibitors in this study have low molecular weight and only one acidic head, and are expected to be good in terms of cell permeability.

Our MD simulations also detect conformational rearrangement of the two-helix lid domain in MptpB, the dynamics characteristics of which will be discussed in detail in the following studies.

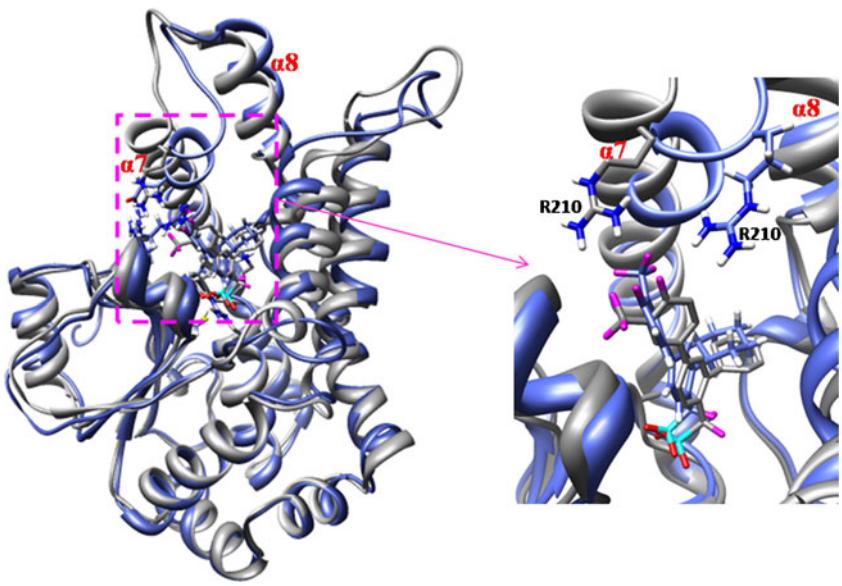

Fig. 6 Rearrangement of the two-helix lid domain in MptpB/DFMP complex after MD simulation. *Gray* Docking structure, *blue* average structure derived from MD simulation

Acknowledgments This work was supported by the National Natural Science Foundation of China (21173129).

References

1. Butler D (2000) New fronts in an old war. Nature 406(6797):670–672
2. Andries K, Verhasselt P, Guillemont J, Gohlmann HWH, Neefs JM, Winkler H, Van Gestel J, Timmerman P, Zhu M, Lee E, Williams P, de Chaffoy D, Huitric E, Hoffner S, Cambau E, Truffot-Pernot C, Lounis N, Jarlier V (2005) A diarylquinoline drug active on the ATP synthase of *Mycobacterium tuberculosis*. Science 307(5707):223–227. doi:10.1126/science.1106753
3. Miller BH, Shinnick TM (2000) Evaluation of *Mycobacterium tuberculosis* genes involved in resistance to killing by human macrophages. Infect Immun 68(1):387–390
4. Beresford NJ, Mulhearn D, Szczepankiewicz B, Liu G, Johnson ME, Fordham-Skelton A, Abad-Zapatero C, Cavet JS, Tabernero L (2009) Inhibition of MptpB phosphatase from *Mycobacterium tuberculosis* impairs mycobacterial survival in macrophages. J Antimicrob Chemother 63(5):928–936. doi:10.1093/Jac/Dkp031
5. Cole ST, Brosch R, Parkhill J, Garnier T, Churcher C, Harris D, Gordon SV, Eiglmeier K, Gas S, Barry CE, Tekaia F, Badcock K, Basham D, Brown D, Chillingworth T, Conner R, Davies R, Devlin K, Feltwell T, Gentles S, Hamlin N, Holroyd S, Hornsby T, Jagels K, Krogh A, McLean J, Moule S, Murphy L, Oliver K, Osborne J, Quail MA, Rajandream MA, Rogers J, Rutter S, Seeger K, Skelton J, Squares R, Squares S, Sulston JE, Taylor K, Whitehead S, Barrell BG (1998) Deciphering the biology of *Mycobacterium tuberculosis* from the complete genome sequence. Nature 393:537–544
6. Koul A, Choidas A, Treder M, Tyagi AK, Drlica K, Singh Y, Ullrich A (2000) Cloning and characterization of secretory tyrosine phosphatases of *Mycobacterium tuberculosis*. J Bacteriol 182 (19):5425–5432
7. Singh R, Rao V, Shakila H, Gupta R, Khera A, Dhar N, Singh A, Koul A, Singh Y, Naseema M, Narayanan PR, Paramasivan CN, Ramanathan VD, Tyagi AK (2003) Disruption of mptpB impairs the ability of *Mycobacterium tuberculosis* to survive in guinea pigs. Mol Microbiol 50(3):751–762. doi:10.1046/j.1365-2958.2003.03712.x
8. Zhou B, He YT, Zhang X, Xu J, Luo Y, Wang YH, Franzblau SG, Yang ZY, Chan RJ, Liu Y, Zheng JY, Zhang ZY (2010) Targeting mycobacterium protein tyrosine phosphatase B for antituberculosis agents. Proc Natl Acad Sci USA 107(10):4573–4578. doi:10.1073/pnas.0909133107
9. Grundner C, Ng HL, Alber T (2005) Mycobacterium tuberculosis protein tyrosine phosphatase PtpB structure reveals a diverged fold and a buried active site. Structure 13(11):1625–1634. doi:10.1016/j.str.2005.07.017
10. Grundner C, Perrin D, van Huijsduijnen RH, Swinnen D, Gonzalez J, Gee CL, Wells TN, Alber T (2007) Structural basis for selective inhibition of *Mycobacterium tuberculosis* protein tyrosine phosphatase PtpB. Structure 15(4):499–509. doi:10.1016/j.str.2007.03.003
11. Beresford N, Patel S, Armstrong J, Szoor B, Fordham-Skelton AP, Tabernero L (2007) MptpB, a virulence factor from *Mycobacterium tuberculosis*, exhibits triple-specificity phosphatase activity. Biochem J 406:13–18
12. Tan LP, Wu H, Yang PY, Kalesh KA, Zhang XH, Hu MY, Srinivasan R, Yao SQ (2009) High-throughput discovery of *Mycobacterium tuberculosis* protein tyrosine phosphatase B (MptpB) inhibitors using click chemistry. Org Lett 11(22):5102–5105. doi:10.1021/Ol9023419
13. Noren-Muller A, Wilk W, Saxena K, Schwalbe H, Kaiser M, Waldmann H (2008) Discovery of a new class of inhibitors of *Mycobacterium tuberculosis* protein tyrosine phosphatase B by biology-oriented synthesis. Angew Chem Int Ed 47(32):5973–5977. doi:10.1002/anie.200801566
14. Correa IR, Noren-Muller A, Ambrosi HD, Jakupovic S, Saxena K, Schwalbe H, Kaiser M, Waldmann H (2007) Identification of inhibitors for mycobacterial protein tyrosine phosphatase B (MptpB) by biology-oriented synthesis (BIOS). Chem Asian J 2 (9):1109–1126. doi:10.1002/asia.200700125
15. Lilienkampf A, Mao JL, Wan BJ, Wang YH, Franzblau SG, Kozikowski AP (2009) Structure-activity relationships for a series of quinoline-based compounds active against replicating and nonreplicating *Mycobacterium tuberculosis*. J Med Chem 52(7):2109–2118. doi:10.1021/Jm900003c
16. Chen L, Zhou B, Zhang S, Wu L, Wang YH, Franzblau SG, Zhang ZY (2010) Identification and characterization of novel inhibitors of mPTPB, an essential virulent phosphatase from *Mycobacterium tuberculosis*. Acs Med Chem Lett 1(7):355–359. doi:10.1021/Ml1001135
17. Soellner MB, Rawls KA, Grundner C, Alber T, Ellman JA (2007) Fragment-based substrate activity screening method for the identification of potent inhibitors of the *Mycobacterium tuberculosis* phosphatase PtpB. J Am Chem Soc 129(31):9613–9615. doi:10.1021/Ja0727520
18. Rawls KA, Grundner C, Ellman JA (2010) Design and synthesis of nonpeptidic, small molecule inhibitors for the *Mycobacterium tuberculosis* protein tyrosine phosphatase PtpB. Org Biomol Chem 8(18):4066–4070. doi:10.1039/C0ob00182a
19. Frisch MJT GW, Schlegel HB, Scuseria GE, Robb MA, Cheeseman JR, Montgomery JY Jr, Vreven T, Kudin KN, Burant JC, Millam JM, Iyengar S, Tomasi J, Barone V, Mennucci B, Cossi M, Scalmani G, Rega N, Petersson GA,Nakatsuji H, Hada M, Ehara M, Toyota K, Fukuda R, Hasegawa J, Ishida M, Nakajima T, Honda Y, Kitao O, Nakai H, Klene M, Li X, Knox JE, Hratchian HP, Cross JB, Bakken V, Adamo C, Jaramillo J, Gomperts R, Stratmann RE, Yazyev O, Austin AJ, Cammi R, Pomelli C, Ochterski JW, Ayala PY, Morokuma K, Voth GA, Salvador P, Dannenberg JJ, Zakrzewski VG, Dapprich S, Daniels AD, Strain MC, Farkas O, Malick DK, Rabuck AJ, Raghavachari K, Foresman JB, Ortiz JV, Cui Q, Baboul AG, Clifford S, Cioslowski J, Stefanov BB, Liu G, Liashenko A, Piskorz P, Komaromi I, Martin RL, Fox DJ, Keith T, Al-Laham MA, Peng CY, Nanayakkara A, Challacombe M, Gill PMW, Johnson B, Chen W, Wong MW, Gonzalez C, Pople JA (2004) Gaussian 03, Revision C. 02. Gaussian, IncWallingford CT
20. Eswar NED, Webb B, Shen MY, Sali A (2008) Protein structure modeling with MODELLER. Methods Mol Biol 426:145–159
21. Liu GX, Tan JZ, Niu CY, Shen JH, Luo XM, Shen X, Chen KX, Jiang HL (2006) Molecular dynamics simulations of interaction between protein-tyrosine phosphatase 1B and a bidentate inhibitor. Acta Pharmacol Sin 27(1):100–110
22. Morris GM, Goodsell DS, Halliday RS, Huey R, Hart WE, Belew RK, Olson AJ (1998) Automated docking using a Lamarckian genetic algorithm and an empirical binding free energy function. J Comput Chem 19(14):1639–1662
23. Sanner MF (1999) Python: a programming language for software integration and development. J Mol Graph Model 17(1):57–61
24. Odzak R, Calic M, Hrenar T, Primozic I, Kovarik Z (2007) Evaluation of monoquaternary pyridinium oximes potency to reactivate tabun-inhibited human acetylcholinesterase. Toxicology 233(1–3):85–96. doi:10.1016/j.tox.2006.08.003
25. Liu GX, Zhang ZS, Luo XM, Shen JH, Liu H, Shen X, Chen KX, Jiang HL (2004) Inhibitory mode of indole-2-carboxamide derivatives against HLGPa: molecular docking and 3D-QSAR analyses. Bioorg Med Chem 12(15):4147–4157. doi:10.1016/j.bmc.2004.05.023
26. Huey R, Morris GM, Olson AJ, Goodsell DS (2007) A semiempirical free energy force field with charge-based desolvation. J Comput Chem 28(6):1145–1152. doi:10.1002/Jcc.20634

27. Van der Spoel D, Lindahl E, Hess B, Groenhof G, Mark AE, Berendsen HJC (2005) GROMACS: Fast, flexible, and free. J Comput Chem 26(16):1701–1718. doi:10.1002/Jcc.20291
28. Lindahl E, Hess B, van der Spoel D (2001) GROMACS 3.0: a package for molecular simulation and trajectory analysis. J Mol Model 7(8):306–317
29. Ito Y, Kondo H, Goldfarb PS, Lewis DFV (2008) Analysis of CYP2D6 substrate interactions by computational methods. J Mol Graph Model 26(6):947–956. doi:10.1016/j.jmgm.2007.07.004
30. Ling BP, Wang ZG, Zhang R, Meng XH, Liu YJ, Zhang CQ, Liu CB (2009) Theoretical studies on the interaction of modified pyrimidines and purines with purine riboswitch. J Mol Graph Model 28(1):37–45. doi:10.1016/j.jmgm.2009.03.005
31. Hornak V, Abel R, Okur A, Strockbine B, Roitberg A, Simmerling C (2006) Comparison of multiple amber force fields and development of improved protein backbone parameters. Proteins Struct Funct Bioinf 65(3):712–725. doi:10.1002/Prot.21123
32. Hess B, Bekker H, Berendsen HJC, Fraaije JGEM (1997) LINCS: A linear constraint solver for molecular simulations. J Comput Chem 18(12):1463–1472
33. Han Y, Belley M, Bayly CI, Colucci J, Dufresne C, Giroux A, Lau CK, Leblanc Y, McKay D, Therien M, Wilson M-C, Skorey K, Chan C-C, Scapin G, Kennedy BP (2008) Discovery of [(3-bromo-7-cyano-2-naphthyl)(difluoro)methyl]phosphonic acid, a potent and orally active small molecule PTP1B inhibitor. Bioorg Med Chem Lett 18(11):3200–3205
34. Wang RX, Lai LH, Wang SM (2002) Further development and validation of empirical scoring functions for structure-based binding affinity prediction. J Comput Aid Mol Des 16:11–26
35. Flynn EM, Hanson JA, Alber T, Yang H (2010) Dynamic active-site protection by the *M. tuberculosis* protein tyrosine phosphatase PtpB lid domain. J Am Chem Soc 132(13):4772–4780. doi:10.1021/Ja909968n